# Diabatic intermolecular potentials and bound states of open-shell atom–molecule dimers: Application to the $F(^2P)-H_2$ complex

W. B. Zeimen,[a] J. Kłos,[b] G. C. Groenenboom,[c] and A. van der Avoird[d]
*Institute of Theoretical Chemistry, NSRIM, University of Nijmegen, Toernooiveld 1, 6525 ED Nijmegen, The Netherlands*

(Received 2 December 2002; accepted 31 January 2003)

We present a general derivation of the expansion of diabatic intermolecular potentials for an open-shell atom interacting with a closed-shell molecule and the multipolar expansion of these potentials in the long range. It is outlined how to compute bound states of the open-shell atom–molecule complex from the set of asymptotically degenerate diabatic potentials in a body-fixed basis of rovibrational wave functions with the inclusion of spin–orbit coupling. This method is applied to produce all the bound energy levels of the $F(^2P)-H_2$ van der Waals complex with recent diabatic potentials obtained from *ab initio* calculations by Kłos *et al.* [Int. J. Quantum Chem. **90**, 1038 (2002)]. The binding energy $D_0$ is 14.6 $cm^{-1}$ for the para-$H_2$ complex and 19.3 $cm^{-1}$ for the ortho-$H_2$ complex. The para-$H_2$–F complex does not possess any bound states for rotational quantum numbers $J$ larger than $\frac{9}{2}$, the ortho-$H_2$–F complex has a maximum $J$ of $\frac{11}{2}$. © *2003 American Institute of Physics.* [DOI: 10.1063/1.1562623]

## I. INTRODUCTION

In the more familiar case of two interacting closed-shell molecules the intermolecular potential obtained by solving the first step of the Born–Oppenheimer (BO) or adiabatic approximation is a scalar function. That is, it is invariant under rotations of the whole system, as well as under space-inversion. When the dependence of the potential on the molecular orientations is expressed by an expansion in a basis of angular functions also these functions should be invariant under overall rotations.[1] Such an expansion is convenient for the application of intermolecular potential surfaces in dynamical calculations, computations of second virial coefficients, etc. The coefficients in the expansion depend on the intermolecular distance $R$ and, for nonrigid molecules, on the intramolecular coordinates.[1,2]

For open-shell systems the situation is more complicated. The electronic states of open-shell atoms and molecules are often degenerate, and for a given electronic state of the interacting species there exists multiple adiabatic intermolecular potential surfaces that are asymptotically degenerate. Nonadiabatic coupling between the electronic states involved becomes important. In dynamical calculations it is useful to define a ''generalized BO model'' which includes the nonadiabatic coupling, but only between the set of electronic states that are asymptotically degenerate. This model works well when the energy separation between the electronic states included in the model and all other states is large with respect to the intermolecular interactions that split the model states.

Formulas for intermolecular potentials between an open-shell atom and a closed-shell diatomic molecule have been presented by Alexander[3] and by Dubernet and Hutson.[4,5] Alexander obtained his formulas[3] by writing the intermolecular interaction operator in the form of the multipole expansion. However, this expansion is valid only in the long range, when there is no overlap between the wave functions of the interacting species. Dubernet and Hutson derived their formulas by starting from the well-known expansion of diatom–diatom potentials, replacing the polar angles of one of the diatom axes by the coordinates of the electrons in the atom, and taking matrix elements with respect to the degenerate electronic substates of the open-shell atom. In Sec. II of this paper we will show that the same formulas can be obtained by defining a general intermolecular potential energy operator $\hat{V}$ for interacting open-shell species and using only the property that this operator is invariant under rotations and inversion. We also define a set of asymptotically degenerate diabatic states and we show how to expand the corresponding diabatic potentials in the appropriate angle-dependent functions. The formulas are first derived for open-shell atom–diatom systems and then generalized to atom–nonlinear molecule systems. Furthermore, it is shown in Sec. III how the diabatic interaction potentials can be expressed in closed analytic form by the use of the multipole expansion that holds in the long range. An important long range interaction term in the coupling potential between diabatic states of the same symmetry was overlooked in Ref. 3.

Next, we outline the procedure to include the set of asymptotically degenerate intermolecular potentials for open-shell atom–molecule dimers in bound state calculations. The theory is applied to the $F(^2P)-H_2(^1\Sigma_g^+)$ complex. The interaction of $F(^2P)$ atoms with $H_2$ molecules has received much attention from experimentalists and theoreticians.[6–21] Most studies address the chemical reaction $F+H_2 \rightarrow H+HF$ or one of its isotopic equivalents, theoretically by quantum

[a]Electronic mail: zeimen@theochem.kun.nl
[b]Electronic mail: jakl@theochem.kun.nl
[c]Electronic mail: gerritg@theochem.kun.nl
[d]Electronic mail: avda@theochem.kun.nl

 

scattering calculations or quasiclassical trajectory studies and experimentally by crossed molecular-beam studies. Theory and experiment have reached a fair level of agreement. In the similar reaction $Cl+H_2 \rightarrow H+HCl$ it was found[22,23] that the occurrence of a weakly bound $Cl-H_2$ complex in the entrance channel of the reaction is of great importance. In the $F+H_2$ reaction the role of such an entrance channel complex $F-H_2$ has not yet been established, but it is certainly worthwhile to study this complex in detail. Lately, Takayanagi and co-workers[24] reported the presence of van der Waals resonances in the $F+H_2$ reaction probability, and they used an approximate approach to calculate $F-H_2$ bound states from one-dimensional effective potential curves. Aquilanti *et al.*[16,17] measured elastic $F-D_2$ scattering cross sections and used these data to construct diabatic $F-H_2$ potential surfaces. Rotationally inelastic $F-H_2$ scattering cross sections were measured in the Toennies group.[19–21]

We report the first detailed study of the bound states of $F-H_2$. We employed the accurate three-dimensional diabatic potential energy surfaces for the F($^2P$)–$H_2$ system that were recently reported by Kłos *et al.*[25] They were obtained from *ab initio* unrestricted coupled cluster calculations with single, double, and noniterative triple excitations [UCCSD(T)]. The *ab initio* data of Kłos *et al.* was refitted (see Sec. IV) with the use of the formulas derived in Secs. II and III. This was necessary because the original fit of this potential had some unphysical artefacts at large distances. These were overlooked in Ref. 25, and they constitute a serious problem in bound state calculations. For comparison, we also computed the bound states of $F-H_2$ from the empirical potentials of Aquilanti *et al.*[17] The method for the calculation of the van der Waals levels on the three asymptotically degenerate diabatic potential energy surfaces with the inclusion of the potential that couples them is presented in Sec. V. The spin–orbit interaction in the F($^2P$) atom is included as well. In Sec. VI we discuss the results.

## II. DIABATIC INTERMOLECULAR POTENTIALS FOR OPEN-SHELL ATOM–MOLECULE COMPLEXES

We consider an open-shell atom (A) interacting with a closed-shell molecule (B). The degenerate states of the open-shell atom A are denoted as $|\lambda,\mu\rangle^{\mathrm{A}}$ with fixed $\lambda$ and $\mu=-\lambda,\ldots,\lambda$. These quantum numbers may refer to the orbital angular momentum of the atom or, more generally, to the total electronic angular momentum $J,M_J$ of a spin–orbit coupled state. In the latter case $\lambda$ can adopt half-integer values. We assume that the states $|\lambda,\mu\rangle^{\mathrm{A}}$ are of well-defined parity $p$ under inversion, $\hat{i}|\lambda,\mu\rangle^{\mathrm{A}}=(-1)^p|\lambda,\mu\rangle^{\mathrm{A}}$. Molecule B is a closed-shell molecule in state $|0\rangle^{\mathrm{B}}$ with no electronic degeneracy. We may define a set of asymptotically degenerate diabatic states of the interacting system A–B and denote these by $|\lambda,\mu\rangle$. Although these wave functions are labeled with the quantum numbers of A, the functions depend on the electronic coordinates of both A and B. For large distance $R$ between A and B they may be written as products $|\lambda,\mu\rangle^{\mathrm{A}}|0\rangle^{\mathrm{B}}$ and the mixing of the diabatic electronic states $|\lambda,\mu\rangle$ of system A–B induced by overall rotation of the whole system follows the transformation of the states $|\lambda,\mu\rangle^{\mathrm{A}}$ of the atom. Since these states are well separated in energy from other electronic states of the interacting system and do not mix with other electronic states, we may assume that this transformation property holds for all relevant distances.

Subsystem B may be a general closed-shell molecule (or atom), but we will first write the formulas for a diatomic molecule. The intermolecular vector $\boldsymbol{R}$ points from the nucleus of atom A to the center-of-mass of molecule B and the vector $\boldsymbol{r}$ is the diatom bond axis. The intermolecular potential energy is a linear operator in the vector space spanned by the set of diabatic states and may be expanded as

$$\hat{V}^{(\lambda)}=\sum_{\mu'\mu}|\lambda,\mu'\rangle^{\mathrm{SF}}\langle\lambda,\mu|V^{(\lambda)}_{\mu'\mu}(R,\beta,\alpha,r,\theta^{\mathrm{SF}},\phi^{\mathrm{SF}}). \quad (1)$$

The functions $V^{(\lambda)}_{\mu'\mu}$ are the diabatic potentials with respect to a space-fixed (SF) coordinate system. They depend on the atom–diatom coordinates: $R$, $\beta$, $\alpha$, the length and the polar angles of the vector $\boldsymbol{R}$ with respect to the SF frame and $r$, $\theta^{\mathrm{SF}}$, $\phi^{\mathrm{SF}}$, the length and polar angles of $\boldsymbol{r}$. These potentials may be expanded

$$V^{(\lambda)}_{\mu'\mu}(R,\beta,\alpha,r,\theta^{\mathrm{SF}},\phi^{\mathrm{SF}}) = \sum_{LQ;ll_{\mathrm{B}}}\mathcal{C}_{(ll_{\mathrm{B}})L,Q}(\beta,\alpha,\theta^{\mathrm{SF}},\phi^{\mathrm{SF}})v^{(\lambda)\mu'\mu}_{ll_{\mathrm{B}};LQ}(R,r) \quad (2)$$

in a complete set of angular functions

$$\mathcal{C}_{(ll_{\mathrm{B}})L,Q}(\beta,\alpha,\theta^{\mathrm{SF}},\phi^{\mathrm{SF}}) = \sum_{mm_{\mathrm{B}}}C_{l,m}(\beta,\alpha)C_{l_{\mathrm{B}},m_{\mathrm{B}}}(\theta^{\mathrm{SF}},\phi^{\mathrm{SF}})\langle l,m;l_{\mathrm{B}},m_{\mathrm{B}}|L,Q\rangle, \quad (3)$$

which are products of two Racah normalized spherical harmonics $C_{l,m}(\theta,\phi)$ coupled by means of Clebsch–Gordan coefficients $\langle l,m;l_{\mathrm{B}},m_{\mathrm{B}}|L,Q\rangle$.[26] The operators $|\lambda,\mu'\rangle\langle\lambda,\mu|$ are also coupled to a Clebsch–Gordan series to produce irreducible tensor operators,

$$\hat{T}^{(\lambda)}_{L',Q'}=\sum_{\mu'\mu}|\lambda,\mu'\rangle\langle\lambda,\mu|(-1)^{\lambda-\mu}\langle\lambda,\mu';\lambda,-\mu|L',Q'\rangle. \quad (4)$$

The above definition holds both with respect to the SF frame and with respect to a body-fixed (BF) frame introduced below. The quantum number $L'$ has always integer values, even if $\lambda$ is a half-integer. From the invariance of the total potential energy operator under overall rotations of the system A–B it follows then that the quantum numbers $L'$ and $Q'$ must be related to the quantum numbers $L$ and $Q$ of the coupled angular expansion functions as $L'=L$ and $Q'=-Q$. The expansion of the rotationally invariant potential energy operator reads

$$\hat{V}^{(\lambda)}=\sum_{LQ}(-1)^Q\hat{T}^{(\lambda)\,\mathrm{SF}}_{L,-Q} \times\sum_{ll_{\mathrm{B}}}\mathcal{C}_{(ll_{\mathrm{B}})L,Q}(\beta,\alpha,\theta^{\mathrm{SF}},\phi^{\mathrm{SF}})v^{(\lambda)}_{ll_{\mathrm{B}};L}(R,r). \quad (5)$$

The choice of rotationally invariant expansion operators implies that the expansion coefficients do not depend on $Q$.

The intermolecular potential depends only on the internal coordinates which can be explicitly defined with the introduction of a body-fixed (BF) frame. A two-angle embedded BF frame is obtained by putting the $z$-axis along the vector $\boldsymbol{R}$, i.e., by rotation of the SF frame over the angles $\beta$, $\alpha$. The diatom axis $\boldsymbol{r}$ has the polar angles $\theta$, $\phi$ in this frame, where $\theta$ is the angle between the vectors $\boldsymbol{R}$ and $\boldsymbol{r}$. A fully embedded BF frame is obtained by a third rotation over the angle $\phi$, which ensures that the diatom axis $\boldsymbol{r}$ lies in the BF $xz$-plane. The coupled angular functions of Eq. (3), when transformed to the BF frame, are given by[2,27]

$$\mathcal{C}_{(ll_B)L,Q}(\beta,\alpha,\theta^{SF},\phi^{SF}) = \sum_K \langle l,0;l_B,K|L,K\rangle D^{(L)}_{Q,K}(\alpha,\beta,\phi)^* C_{l_B,K}(\theta,0). \quad (6)$$

The function $D^{(L)}_{Q,K}(\alpha,\beta,\phi)$ is an element of the Wigner rotation matrix.[26] The diabatic basis $|\lambda,\mu\rangle$ and the irreducible tensors in Eq. (4) transform from the SF to the BF frame by the standard rotation rules. Substitution of these results into Eq. (5) and use of the properties[26] of Wigner $D$-functions yields the expansion of the potential with respect to the BF frame,

$$\hat{V}^{(\lambda)} = \sum_{LK} \hat{T}^{(\lambda)^{BF}}_{L,-K} \sum_{l_B} C_{l_B,K}(\theta,0) v^{(\lambda)}_{l_B;L,K}(R,r). \quad (7)$$

The expansion coefficients in Eq. (7) are related to those in Eq. (5) as

$$v^{(\lambda)}_{l_B;L,K}(R,r) = (-1)^K \sum_l \langle l,0;l_B,K|L,K\rangle v^{(\lambda)}_{ll_B;L}(R,r). \quad (8)$$

The diabatic potentials that occur in a nonadiabatic dynamical treatment according to the ''generalized BO model'' are the matrix elements of the rotationally invariant potential energy operator $\hat{V}^{(\lambda)}$ over the diabatic states $|\lambda,\mu\rangle$ with $\mu=-\lambda,\ldots,\lambda$. They are most conveniently expressed in BF coordinates. With the aid of Eq. (4) it follows from Eq. (7) that the diabatic potentials can be expanded as

$$V^{(\lambda)}_{\mu',\mu}(R,r,\theta) = \langle \lambda,\mu'|\hat{V}^{(\lambda)}|\lambda,\mu\rangle^{BF} = \sum_{l_B} C_{l_B,\mu-\mu'}(\theta,0) v^{(\lambda)\mu',\mu}_{l_B}(R,r) \quad (9)$$

with coefficients

$$v^{(\lambda)\mu',\mu}_{l_B}(R,r) = \sum_{LK} (-1)^{\lambda-\mu} \langle \lambda,\mu';\lambda,-\mu|L,-K\rangle \times v^{(\lambda)}_{l_B;L,K}(R,r). \quad (10)$$

Only terms with $K=\mu-\mu'$ occur in this summation and the expansion of a given diabatic potential $V^{(\lambda)}_{\mu',\mu}(R,r,\theta)$ in Eq. (9) contains only spherical harmonics $C_{l_B,K}(\theta,0)$ with $K=\mu-\mu'$. The index $l_B$ runs from $|K|$ to infinity.

We also require that the potential energy operator is invariant under inversion, $\hat{i}\hat{V}^{(\lambda)}\hat{i}^\dagger = \hat{V}^{(\lambda)}$. The effect of inversion on the BF diabatic states is given in Ref. 28 (Sec. V in the Appendix). The irreducible tensor operators defined in Eq. (4) behave under inversion as $\hat{i}\hat{T}^{(\lambda)^{BF}}_{L,Q}\hat{i}^\dagger = (-1)^{L-Q}\hat{T}^{(\lambda)^{BF}}_{L,-Q}$. The angle $\theta$ does not change by inversion and the real angular functions in Eq. (7) obey the relation $C_{l_B,-K}(\theta,0) = (-1)^K C_{l_B,K}(\theta,0)$. When we apply inversion invariance to the expansion of the potential energy operator in Eq. (7) and use these relations, it becomes clear that the expansion coefficients must satisfy

$$v^{(\lambda)}_{l_B;L,-K}(R,r) = (-1)^L v^{(\lambda)}_{l_B;L,K}(R,r). \quad (11)$$

Then, with the aid of Eq. (10), one can show that the expansion coefficients of the diabatic potentials in Eq. (9) have the property,

$$v^{(\lambda)-\mu',-\mu}_{l_B}(R,r) = v^{(\lambda)\mu',\mu}_{l_B}(R,r). \quad (12)$$

Finally, from the requirement that the potential energy operator $\hat{V}^{(\lambda)}$ must be Hermitian it follows that

$$v^{(\lambda)}_{l_B;L,K}(R,r)^* = v^{(\lambda)}_{l_B;L,-K}(R,r) \quad (13)$$

and the expansion coefficients of the diabatic potentials in Eq. (9) obey the additional relation,

$$v^{(\lambda)\mu',\mu}_{l_B}(R,r)^* = (-1)^{\mu'-\mu} v^{(\lambda)\mu,\mu'}_{l_B}(R,r). \quad (14)$$

Instead of the diabatic wave functions $|\lambda,\mu\rangle^{BF}$ one may use wave functions that are even or odd with respect to inversion $\hat{i}$. This paper deals with atom–diatom systems, the diabatic states $|\lambda,\mu\rangle$ are pure orbital angular momentum states, and the quantum number $\lambda$ adopts integer values only. In the Appendix of Ref. 28 it is shown that inversion with respect to the SF system is equivalent to the operation $\hat{R}_y(\pi)\hat{i}$ in the BF system. For purely spatial wave functions this operation is a reflection $\sigma_{xz}$ with respect to the plane through the nuclei. It follows directly that the combinations

$$|0\rangle = |\lambda,0\rangle^{BF} \quad \text{for } p+\lambda \text{ even}$$
$$|\mu+\rangle = (|\lambda,-\mu\rangle^{BF} + (-1)^{p+\lambda-\mu}|\lambda,\mu\rangle^{BF})/\sqrt{2}$$

$A'$ symmetry

$$|0\rangle = |\lambda,0\rangle^{BF} \quad \text{for } p+\lambda \text{ odd}$$
$$|\mu-\rangle = i(|\lambda,-\mu\rangle^{BF} - (-1)^{p+\lambda-\mu}|\lambda,\mu\rangle^{BF})/\sqrt{2}$$

$A''$ symmetry (15)

(with $\mu>0$) are symmetric ($A'$) or antisymmetric ($A''$) under this reflection $\sigma_{xz}$. If the atom is in a $P$ state, then $\lambda=1$ and $\mu=-1,\ 0,\ 1$. For linear geometries ($\theta=0$) the first function of $A'$ symmetry describes a $\Sigma$ state with respect to the intermolecular axis $\boldsymbol{R}$. The second function of $A'$ symmetry and the function of $A''$ symmetry form the components of a twofold degenerate $\Pi$ state. With the aid of Eqs. (12) and (14) one finds that the matrix elements, i.e., the diabatic potentials, in this basis are related (for $p+\lambda$ even) to the matrix elements in Eq. (9) by

$$\begin{aligned}
&\langle 0|\hat{V}^{(\lambda)}|0\rangle=\langle\lambda,0|\hat{V}^{(\lambda)}|\lambda,0\rangle^{\mathrm{BF}},\\
&\langle\mu'+|\hat{V}^{(\lambda)}|\mu+\rangle=(-1)^{\mu'+\mu}\langle\lambda,\mu'|\hat{V}^{(\lambda)}|\lambda,\mu\rangle^{\mathrm{BF}}\\
&\qquad\qquad+(-1)^{p+\lambda-\mu'}\langle\lambda,\mu'|\hat{V}^{(\lambda)}|\lambda,-\mu\rangle^{\mathrm{BF}},\\
&\langle 0|\hat{V}^{(\lambda)}|\mu+\rangle=(-1)^{p+\lambda-\mu}\sqrt{2}\langle\lambda,0|\hat{V}^{(\lambda)}|\lambda,\mu\rangle^{\mathrm{BF}},\\
&\langle\mu'+|\hat{V}^{(\lambda)}|\mu-\rangle=0,\\
&\langle 0|\hat{V}^{(\lambda)}|\mu-\rangle=0,\\
&\langle\mu'-|\hat{V}^{(\lambda)}|\mu-\rangle=(-1)^{\mu'+\mu}\langle\lambda,\mu'|\hat{V}^{(\lambda)}|\lambda,\mu\rangle^{\mathrm{BF}}\\
&\qquad\qquad-(-1)^{p+\lambda-\mu'}\langle\lambda,\mu'|\hat{V}^{(\lambda)}|\lambda,-\mu\rangle^{\mathrm{BF}}.
\end{aligned}\tag{16}$$

So, when the diabatic states are adapted to symmetry $A'$ and $A''$ the matrix $\boldsymbol{V}^{(\lambda)}(R,r,\theta)$ with elements given by the diabatic potentials becomes block-diagonal, with a $2\times2$ block of $A'$ symmetry and a single matrix element of $A''$ symmetry. For odd values of $p+\lambda$ the state $|\lambda,0\rangle^{\mathrm{BF}}$ is of $A''$ symmetry and the nonzero matrix elements of this symmetry form a $2\times2$ block, while the $A'$ symmetry block contains only one element in that case. Adiabatic potentials are, by definition, the eigenvalues of this matrix. The adiabatic states have either $A'$ or $A''$ symmetry and can be obtained by separate diagonalizations of the corresponding symmetry blocks.

Sometimes (see Sec. V) it is convenient to use the two-angle embedded BF frame instead of the BF frame obtained by the rotation $\hat{R}(\alpha,\beta,\phi)$. Such a frame is obtained by the rotation $\hat{R}(\alpha,\beta,0)$ that directs the BF $z$-axis along the vector $\boldsymbol{R}$. The irreducible tensor operators that correspond to the diabatic states in these two BF systems are related as

$$\hat{T}^{(\lambda)\,\mathrm{BF}}_{L,-K}=\exp(iK\phi)\hat{T}^{(\lambda)\,\mathrm{BF},2}_{L,-K}.\tag{17}$$

This additional factor depending on the angle $\phi$ can be put into the spherical harmonics $C_{l_\mathrm{B},K}(\theta,0)$ in Eq. (7). Recalling that Eq. (10) yields $K=\mu-\mu'$ one finds that the expansion of the diabatic potentials

$$\begin{aligned}
V^{(\lambda)}_{\mu',\mu}(R,r,\theta,\phi)&=\langle\lambda,\mu'|\hat{V}^{(\lambda)}|\lambda,\mu\rangle^{\mathrm{BF},2}\\
&=\sum_{l_\mathrm{B}}C_{l_\mathrm{B},\mu-\mu'}(\theta,\phi)v^{(\lambda)\mu',\mu}_{l_\mathrm{B}}(R,r)
\end{aligned}\tag{18}$$

differs only slightly from the expansion in Eq. (9) for the fully BF system.

When molecule B is a general nonlinear molecule instead of a diatom we write $\boldsymbol{q}$ for the internal coordinates instead of $r$. The diatom axis $\boldsymbol{r}$ must be replaced by one of the molecule's principal axes, preferentially a symmetry axis (if present). An extra angle $\chi$ is needed to define the orientation of the molecule with respect to the BF frame. This angle corresponds to the rotation of the molecule about the principal axis chosen. When the molecule is a symmetric top its rotational states are labeled with an extra quantum number $k_\mathrm{B}$, but also for a general nonlinear molecule the symmetric rotor functions labeled with $(l_\mathrm{B},m_\mathrm{B},k_\mathrm{B})$ form a basis. The expansion of the intermolecular potential requires an extra summation over $k_\mathrm{B}$. This quantum number is a spectator quantum number that is not involved in the angular momentum coupling. We obtain the same formula for the BF expansion of the diabatic potentials as in Eq. (18), except for the Racah spherical harmonics $C_{l_\mathrm{B},K}(\theta,\phi)$ that must be replaced by Wigner rotation functions $D^{(l_\mathrm{B})}_{K,k_\mathrm{B}}(\phi,\theta,\chi)^*$,

$$\begin{aligned}
V^{(\lambda)}_{\mu',\mu}(R,\boldsymbol{q},\phi,\theta,\chi)&=\langle\lambda,\mu'|\hat{V}^{(\lambda)}|\lambda,\mu\rangle^{\mathrm{BF},2}\\
&=\sum_{l_\mathrm{B},k_\mathrm{B}}D^{(l_\mathrm{B})}_{\mu-\mu',k_\mathrm{B}}(\phi,\theta,\chi)^*\,v^{(\lambda)\mu',\mu}_{l_\mathrm{B},k_\mathrm{B}}(R,\boldsymbol{q}).
\end{aligned}\tag{19}$$

## III. LONG RANGE INTERACTIONS

For large distances $R$ between the atom A and the (general) molecule B we can write the diabatic wave functions as $|\lambda,\mu\rangle^\mathrm{A}|0\rangle^\mathrm{B}$. For the intermolecular interaction operator $\hat{V}$ we can use the multipole expansion in spherical tensor form.[1] The diabatic potentials in the long range region are obtained by taking the $(2\lambda+1)$-dimensional matrix of the operator $\hat{V}$ over the diabatic basis $|\lambda,\mu\rangle^\mathrm{A}|0\rangle^\mathrm{B}$ with $\mu=-\lambda,\ldots,\lambda$. The matrix elements[29] contain the atomic integrals $\langle\lambda,\mu'|\hat{Q}^{(l_\mathrm{A})}_{m_\mathrm{A}}|\lambda,\mu\rangle^\mathrm{A}$ over the components ($m_\mathrm{A}=-l_\mathrm{A},\ldots,l_\mathrm{A}$) of the multipole operator $\hat{Q}^{(l_\mathrm{A})}_{m_\mathrm{A}}$ with the basis $|\lambda,\mu\rangle^\mathrm{A}$ on the open-shell atom A. These integrals can all be expressed in terms of a single atomic multipole moment $Q^{(l_\mathrm{A})}=\langle\lambda,0|\hat{Q}^{(l_\mathrm{A})}_0|\lambda,0\rangle^\mathrm{A}$ by means of the Wigner–Eckart theorem.[26] They also contain expectation values of the multipole operators $\hat{Q}^{(l_\mathrm{B})}_{k_\mathrm{B}}$ over the ground state wave function $|0\rangle^\mathrm{B}$, which are the permanent multipole moments $Q^{(l_\mathrm{B})}_{k_\mathrm{B}}$ of molecule B. These multipole moments $Q^{(l_\mathrm{B})}_{k_\mathrm{B}}$ are defined with respect to a reference frame on monomer B and are given with respect to the dimer BF frame by the equation $\tilde{Q}^{(l_\mathrm{B})}_{m_\mathrm{B}}=\Sigma_{k_\mathrm{B}}Q^{(l_\mathrm{B})}_{k_\mathrm{B}}D^{(l_\mathrm{B})}_{m_\mathrm{B},k_\mathrm{B}}(\phi,\theta,\chi)^*$. The Euler angles ($\phi$, $\theta$, $\chi$) relate the monomer frame on B to the two-angle embedded dimer BF frame. Finally, the multipole expansion contains spherical harmonics $C_{l_\mathrm{A}+l_\mathrm{B},-m_\mathrm{A}-m_\mathrm{B}}(\beta,\alpha)$, which in the dimer BF frame with its $z$-axis along the vector $\boldsymbol{R}$ are simply $C_{l_\mathrm{A}+l_\mathrm{B},-m_\mathrm{A}-m_\mathrm{B}}(0,0)=\delta_{m_\mathrm{A}+m_\mathrm{B},0}$. Substitution of the above relations into the multipole expanded diabatic potentials yields precisely Eq. (19) with expansion coefficients expressed in closed form

$$v_{l_B,k_B}^{(\lambda)\mu',\mu}(R,\boldsymbol{q})=\sum_{l_A}\left[\frac{(2l_A+2l_B+1)!}{(2l_A)!(2l_B)!}\right]^{1/2}(-1)^{l_A-\mu'}\times\begin{pmatrix} l_A & l_B & l_A+l_B \\ \mu'-\mu & \mu-\mu' & 0\end{pmatrix}\times\begin{pmatrix} \lambda & l_A & \lambda \\ -\mu' & \mu'-\mu & \mu\end{pmatrix}\times\begin{pmatrix} \lambda & l_A & \lambda \\ 0 & 0 & 0\end{pmatrix}^{-1}Q^{(l_A)}Q_{k_B}^{(l_B)}R^{-l_A-l_B-1}. \tag{20}$$

The quantities in large round brackets are 3-$j$ symbols. Note that the molecular multipole moments $Q_{k_B}^{(l_B)}$ depend on the internal coordinates $\boldsymbol{q}$ of B. For linear molecules B only terms with $k_B=0$ are present and one obtains the expansion of Eq. (9).

For atom A in a $P$ state, such as F($^2P$), Cl($^2P$), Br($^2P$), the only nonvanishing multipole moment is the quadrupole $Q_A$, with $l_A=2$. When B is a linear molecule with dipole $d_B$ and quadrupole $Q_B$ the dipole–quadrupole interaction matrix for the diabatic basis $|\lambda,\mu\rangle^{BF}$ with $\lambda=1$ and $\mu=-1, 0, 1$ is

$$\boldsymbol{V}^{dq}=\begin{bmatrix} \frac{3}{2}P_{1,0} & \frac{3}{4}P_{1,1}\sqrt{2} & 0 \\ \frac{3}{4}P_{1,1}\sqrt{2} & -3\,P_{1,0} & -\frac{3}{4}P_{1,1}\sqrt{2} \\ 0 & -\frac{3}{4}P_{1,1}\sqrt{2} & \frac{3}{2}P_{1,0}\end{bmatrix}\frac{Q_A d_B}{R^4} \tag{21}$$

with the associated Legendre functions $P_{1,0}=\cos\theta$ and $P_{1,1}=\sin\theta$. The quadrupole–quadrupole interaction matrix is

$$\boldsymbol{V}^{qq}=\begin{bmatrix} -3P_{2,0} & -P_{2,1}\sqrt{2} & -\frac{1}{4}P_{2,2} \\ -P_{2,1}\sqrt{2} & 6P_{2,0} & P_{2,1}\sqrt{2} \\ -\frac{1}{4}P_{2,2} & P_{2,1}\sqrt{2} & -3P_{2,0}\end{bmatrix}\frac{Q_A Q_B}{R^5} \tag{22}$$

with the associated Legendre functions $P_{2,0}=\frac{1}{2}(3\cos^2\theta-1)$, $P_{2,1}=3\sin\theta\cos\theta$, and $P_{2,2}=3\sin^2\theta$.

For the diabatic basis $|0\rangle$, $|1+\rangle$, and $|1-\rangle$ adapted to inversion symmetry and with the assumption that $|0\rangle$ is of even parity the dipole–quadrupole interaction matrix is

$$\boldsymbol{V}^{dq}=\begin{bmatrix} -3P_{1,0} & \frac{3}{2}P_{1,1} & 0 \\ \frac{3}{2}P_{1,1} & \frac{3}{2}P_{1,0} & 0 \\ 0 & 0 & \frac{3}{2}P_{1,0}\end{bmatrix}\frac{Q_A d_B}{R^4}. \tag{23}$$

The quadrupole–quadrupole interaction matrix in the symmetry-adapted basis is

$$\boldsymbol{V}^{qq}=\begin{bmatrix} 6P_{2,0} & -2P_{2,1} & 0 \\ -2P_{2,1} & -3P_{2,0}+\frac{1}{4}P_{2,2} & 0 \\ 0 & 0 & -3P_{2,0}-\frac{1}{4}P_{2,2}\end{bmatrix}\frac{Q_A Q_B}{R^5}. \tag{24}$$

Observe that the off-diagonal matrix element $V_{12}$, called $V_{xz}$ in Ref. 3, contains important long-range contributions which were overlooked in that reference.

## IV. REFIT OF THE *AB INITIO* DATA

Three-dimensional diabatic potentials for F($^2P$)–$H_2$ were calculated in Ref. 25. After careful checking we found, however, that the analytical fit of these potentials given in Ref. 25 revealed unphysical behavior in the region with $R>5.5$ Å not covered by the *ab initio* calculations. Since this behavior would cause problems in the calculation of bound van der Waals levels we decided to refit the *ab initio* data for $V_{0,0}^{(\lambda)}$, $V_{1,1}^{(\lambda)}=V_{-1,-1}^{(\lambda)}$ and $V_{1,-1}^{(\lambda)}=V_{-1,1}^{(\lambda)}$. The $V_{0,1}^{(\lambda)}$ diabatic surface of Ref. 25 behaves correctly and was kept. The quantum number $\lambda$ is always 1 in the remainder of this paper and from here on will be omitted from the notation of the potentials. Note that $-1\leqslant\mu,\mu'\leqslant 1$.

The *ab initio* calculation of the potentials in Ref. 25 was performed for linear and T-shaped F–$H_2$ for a range of distances $R$ and $r$. Three adiabatic (clamped nuclei) potential surfaces were obtained for each of these geometries. For the linear geometry these were labeled $V^{\Sigma}$ and $V^{\Pi}$, the latter being twofold degenerate. For the T-shaped geometry they were labeled $V^{A_1}$, $V^{B_1}$, and $V^{B_2}$ according to their $C_{2v}$ symmetry. The procedure to fit the $R$ and $r$ dependence of the potentials $V^s(R,r)$ for each of these symmetries $s$ was previously applied to the Cl–$H_2$ van der Waals complex and described in detail in Ref. 30. Briefly, the *ab initio* points for each value of $r$ were fitted to the Esposti–Werner[31] functions of the variable $R$,

$$V(R)=G(R)\exp(-a_1R-a_2)-T(R)\sum_{n=5}^{9}C_nR^{-n}, \tag{25}$$

where

$$G(R)=\sum_{j=0}^{8}g_jR^j \tag{26}$$

and

$$T(R)=\tfrac{1}{2}(1+\tanh(1+tR)) \tag{27}$$

is a damping function. The parameters $a_i$, $g_j$, $t$, and $C_n$ were optimized for each value of $r$ with the modified Levenberg–Marquardt algorithm from the MINPACK set of routines for nonlinear least squares fitting. The smallest root mean square (rms) value of the fit was on the order of 0.001 $cm^{-1}$ and usually the rms did not exceed 0.1 $cm^{-1}$. Then the potentials $V^s(R,r)$ for each symmetry $s=\Sigma$, $\Pi$, $A_1$, $B_1$, $B_2$ were expanded in a power series of fractional extensions $z=(r-r_e)/r_e$ of the $H_2$ bond length with respect to the equilibrium value $r_e=1.400\ a_0$,

$$V^s(R,r)=\sum_{p=0}^{4}v_p^s(R)z^p. \tag{28}$$

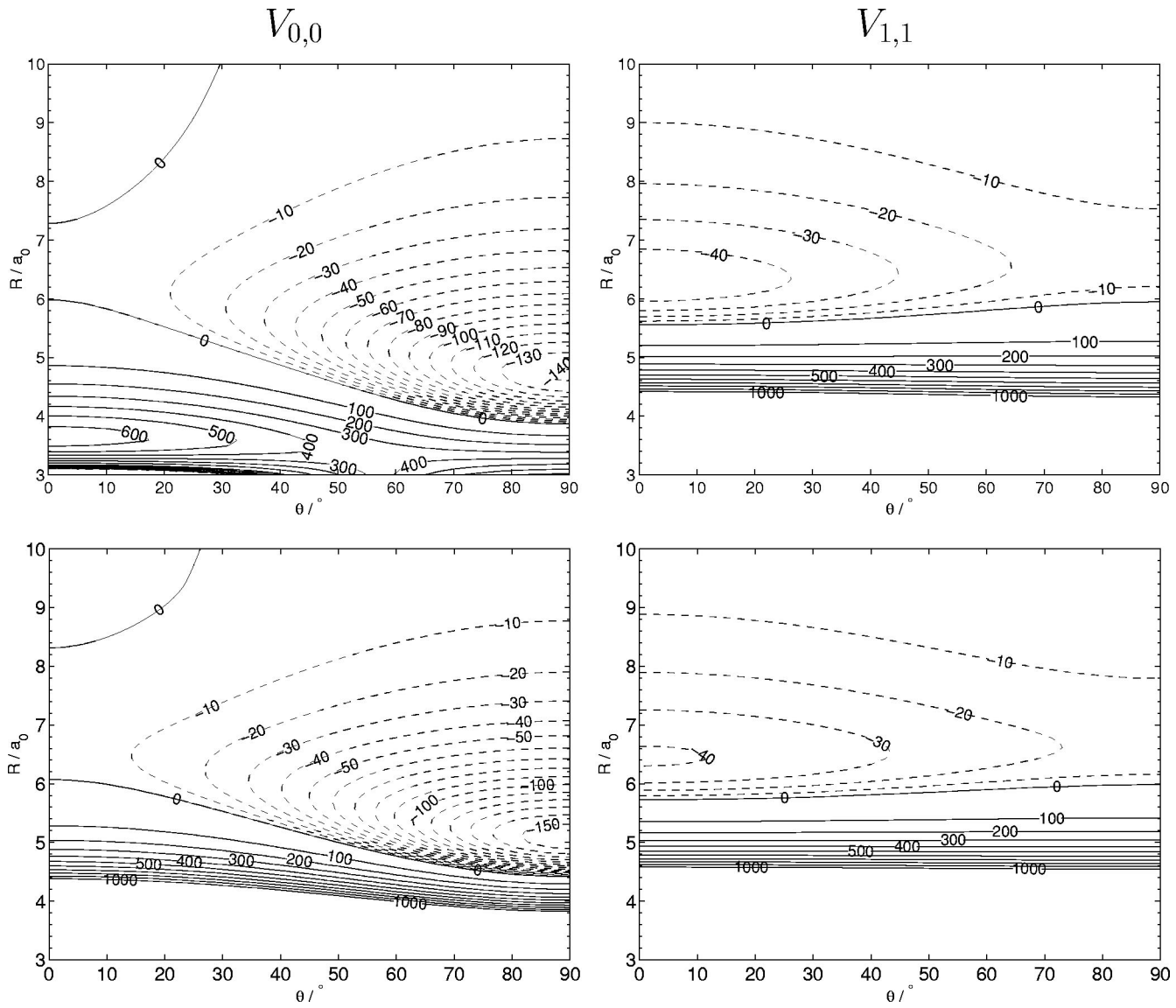


FIG. 1. Contour plots of the diabatic potentials $V_{0,0}$ and $V_{1,1}=[V_{1+,1+}+V_{1-,1-}]/2$. Upper panels: Kłos *et al.* (Ref. 25) and this paper. Lower panels: Aquilanti *et al.* (Ref. 17).

Results for $V^s(R,r)$ were available for four values of $z$ (in addition to $z=0$) and to obtain the coefficients $v_p^s(R)$ for a given value of $R$ we solved a system of four linear equations.

At the linear ($\theta=0°$) and T-shaped ($\theta=90°$) geometries, where the *ab initio* calculations were made, the symmetry is higher than the general $C_s$ symmetry of the planar triatomic species that was used to adapt the diabatic states according to their reflection ($A'$ or $A''$) behavior, see Eq. (15). The $\Sigma$ state and the in-plane $\Pi$ state of the linear geometry obtain $A'$ symmetry when the system is bent and the out-of-plane $\Pi$ state obtains $A''$ symmetry. For the T-shaped ($C_{2v}$) geometry the $A_1$ and $B_2$ states correlate with $A'$ symmetry in $C_s$ and the $B_1$ state with $A''$ symmetry. Because of the higher symmetry at these specific geometries there is no coupling between the two diabatic states of $A'$ symmetry, i.e., the coupling potential $V_{0,1}(R,r,\theta)$ must vanish for $\theta=0°$ and 90°, cf. Eq. (16). Therefore, the diabatic states at these geometries are the same as the adiabatic states. For the linear geometry the diabatic potentials $V_{0,0}$ and $V_{1+,1+}$ of $A'$ symmetry correspond to the adiabatic potentials $V^{\Sigma}$ and $V^{\Pi}$, respectively, and the diabatic potential $V_{1-,1-}$ of $A''$ symmetry also corresponds to $V^{\Pi}$. For the T-shaped geometry the two diabatic potentials of $A'$ symmetry correspond to the adiabatic potentials $V^{A_1}$ and $V^{B_2}$ and the $A''$ diabatic potential to $V^{B_1}$.

The expansion of the diabatic potentials $V_{\mu',\mu}(R,r,\theta)$ in Racah normalized spherical harmonics $C_{l_B,\mu-\mu'}(\theta,0)$ is given in Eq. (9). Only terms with even values of $l_B$ occur in this expansion because $H_2$ is homonuclear. On the basis of experience with rare gas–$H_2$ complexes[32–35] the terms with $l_B \geqslant 4$ in this expansion may be neglected. When the terms with $l_B=0$ and $l_B=2$ are substituted into the right-hand side of Eq. (16) with the values of the Racah spherical harmonics $C_{l_B,\mu-\mu'}(\theta,0)$ at $\theta=0°$ and $\theta=90°$ for the linear and T-shaped geometries, respectively, the diabatic potentials of

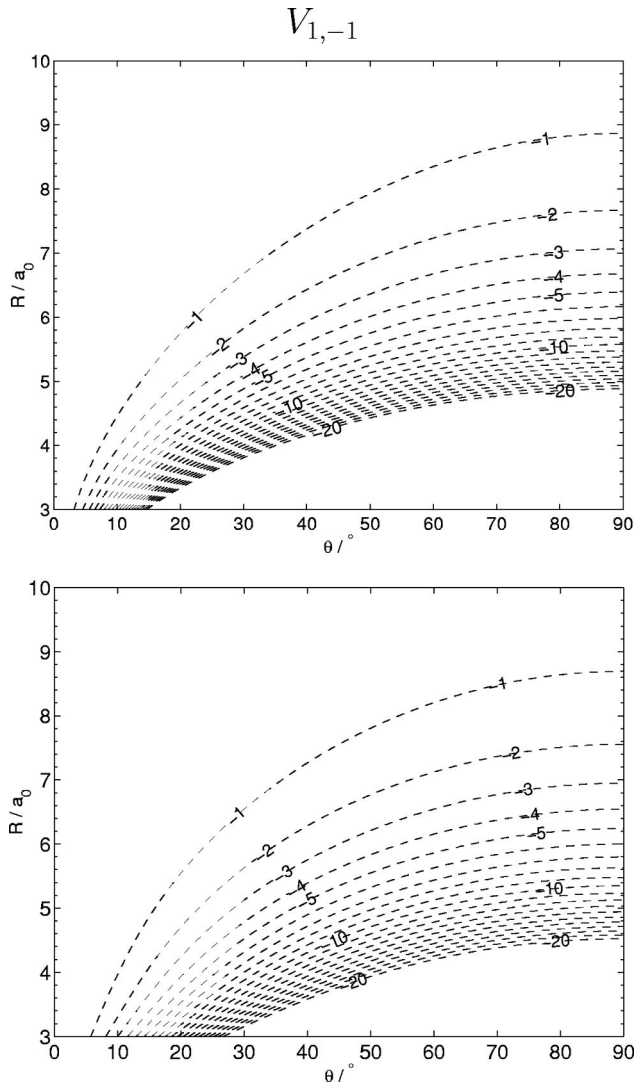


FIG. 2. Contour plots of the diabatic potential $V_{1,-1}=[V_{1+,1+}-V_{1-,1-}]/2$. Upper panel: Kłos *et al.* (Ref. 25) and this paper. Lower panel: Aquilanti *et al.* (Ref. 17).

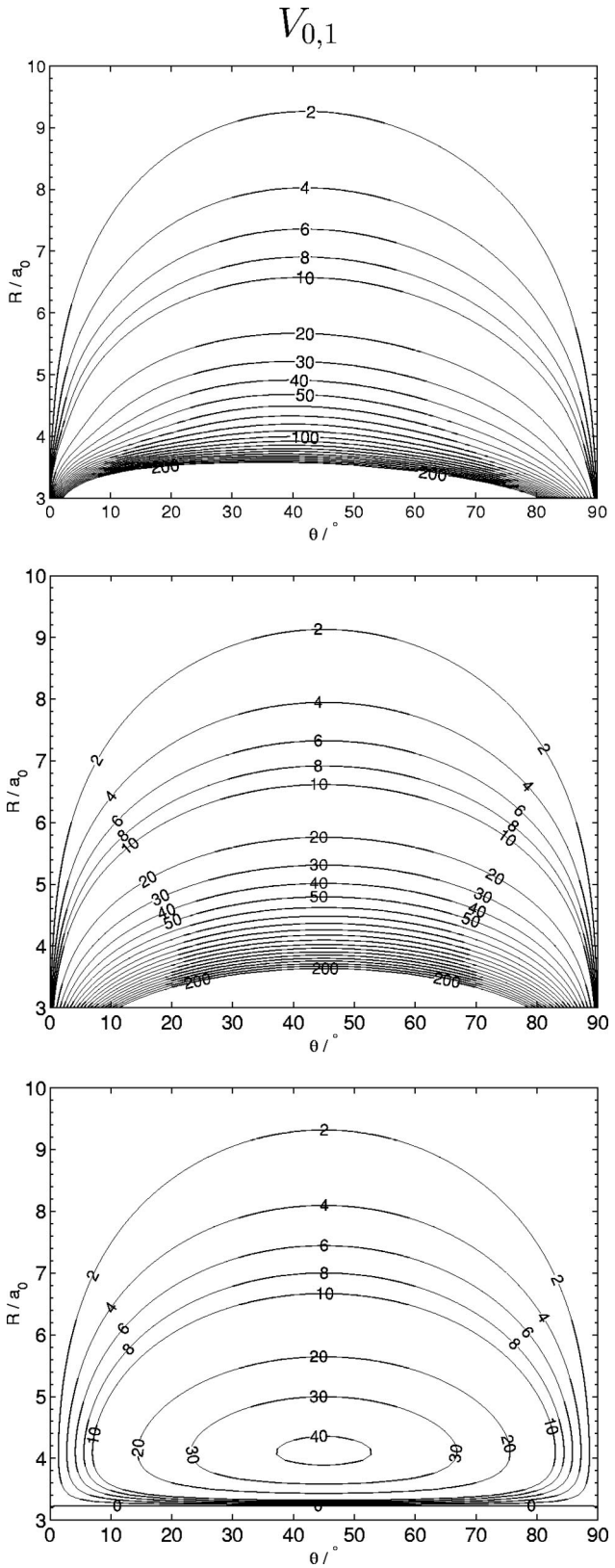


FIG. 3. Contour plots of the diabatic coupling potential $V_{0,1}=-V_{0,1+}/\sqrt{2}$. Top panel: Kłos *et al.* (Ref. 25) and this paper. Middle panel: Long range quadrupole–quadrupole term only. Bottom panel: Aquilanti *et al.* (Ref. 17).

$A'$ and $A''$ symmetry become simple linear combinations of the expansion coefficients $v_{l_B}^{\mu',\mu}(R,r)$. Setting these potentials equal to the corresponding adiabatic potentials and using the symmetry relations for the expansion coefficients [Eqs. (12) and (14)] gives simple sets of linear equations that are easily solved to find

$$v_0^{0,0}(R,r)=\tfrac{1}{3}[2V^{A_1}(R,r)+V^{\Sigma}(R,r)],$$

$$v_2^{0,0}(R,r)=\tfrac{2}{3}[V^{\Sigma}(R,r)-V^{A_1}(R,r)], \tag{29}$$

$$v_0^{1,1}(R,r)=v_0^{-1,-1}(R,r)=\tfrac{1}{3}[V^{B_1}(R,r)+V^{B_2}(R,r)+V^{\Pi}(R,r)],$$

$$v_2^{1,1}(R,r)=v_2^{-1,-1}(R,r)=\tfrac{1}{3}[2V^{\Pi}(R,r)-V^{B_1}(R,r)+V^{B_2}(R,r)], \tag{30}$$

$$v_2^{1,-1}(R,r)=v_2^{-1,1}(R,r)=\frac{2}{\sqrt{6}}[V^{B_1}(R,r)-V^{B_2}(R,r)]. \quad (31)$$

Hence, the expansion coefficients of the diabatic potentials $V_{\mu',\mu}(R,r,\theta)$ can be directly obtained from the fitted adiabatic potentials $V^s(R,r)$.

The diabatic coupling potential $V_{0,1}(R,r,\theta)=-V_{-1,0}(R,r,\theta)=V_{1,0}(R,r,\theta)=-V_{0,-1}(R,r,\theta)$ cannot be extracted from these calculations, because it vanishes both at the linear and T-shaped geometries. It was calculated for a number of angles $\theta$ and expanded in spherical harmonics $C_{l_B,1}(\theta,0)$ by means of Gauss–Legendre quadrature. Note, however, that the potential expanded in Ref. 25 refers to a diabatic basis adapted to symmetry $A'$ and $A''$ and corresponds to the matrix element $V_{0,1+}(R,r,\theta)$ of Eq. (16). Equation (16) shows that $V_{0,1}(R,r,\theta)=-V_{0,1+}(R,r,\theta)/\sqrt{2}$.

The refitted potentials are plotted in Figs. 1, 2, and 3. They are free from artifacts in the long range and can be safely used in bound state calculations. They are available upon request from Kłos; also requests for the potential from Ref. 25 will be fulfilled by sending the refitted ones. In these figures we also plotted the empirical potentials of Aquilanti *et al.*[17] obtained from elastic F–$H_2$ scattering cross sections. The diabat $V_{0,0}$ has a global minimum for the T-shaped geometry. In our potential the position of this minimum is at $R_e=2.49$ Å with well depth $D_e=141.4$ cm$^{-1}$, whereas in the potential of Aquilanti *et al.* this minimum occurs at $R_e=2.69$ Å and is deeper with $D_e=157.03$ cm$^{-1}$. The global minimum in the diabat $V_{1,1}$ occurs for the collinear geometry. In our potential this minimum is located at $R_e=3.35$ Å with $D_e=46.76$ cm$^{-1}$, while the potential of Aquilanti *et al.* has its minimum at $R_e=3.42$ Å with $D_e=41.05$ cm$^{-1}$. The diabat $V_{1,-1}$ in Fig. 2 is the small difference $[V_{1+,1+}-V_{1-,1-}]/2$. Also this diabat is quite similar for the two potentials. The off-diagonal coupling term $V_{0,1}$ in Fig. 3 again shows larger differences between our potential and that of Aquilanti *et al.* Comparison of the upper two panels of this figure makes it clear that the behavior of this diabatic coupling potential is completely dominated by the long range quadrupole–quadrupole interaction [see Eq. (22)] a contribution that was overlooked in Ref. 3.

## V. BOUND STATE CALCULATIONS

The bound state calculations on F($^2P$)–$H_2$ are most conveniently performed in a two-angle embedded BF frame with the $z$-axis along the vector $\boldsymbol{R}$ from the F-atom to the $H_2$ center of mass. The H–H bond axis $\boldsymbol{r}$ has the polar angles ($\theta$, $\phi$) with respect to this frame. The $H_2$ vibration is very fast and can be adiabatically separated from the intermolecular motions in the F–$H_2$ complex. Actually, which is almost equivalent,[36] we froze the H–H bond length at its ground state vibrationally averaged value $r=1.448\,36\ a_0$ and used the vibrationally averaged value $b_0=59.336\,322$ cm$^{-1}$ of the $H_2$ rotational constant. For comparison we also performed some calculations with the potential averaged over the $H_2$ ground state ($v=0$) vibration and with the H–H bond length frozen at its equilibrium value $r_e=1.401\,12\ a_0$ and $b_e=60.853\,119$ cm$^{-1}$.

In the two-angle BF representation the nuclear motion Hamiltonian reduces to

$$\hat{H}=\frac{-\hbar^2}{2\mu_{AB}R}\frac{\partial^2}{\partial R^2}R+\frac{(\hat{\boldsymbol{j}}_A+\hat{\boldsymbol{j}}_B)^2-2(\hat{\boldsymbol{j}}_A+\hat{\boldsymbol{j}}_B)\cdot\hat{\boldsymbol{J}}+\hat{J}^2}{2\mu_{AB}R^2}$$
$$+b_0\hat{j}_B^2+A\hat{\boldsymbol{\lambda}}\cdot\hat{\boldsymbol{S}}+\sum_{\mu',\mu}|\lambda,\mu'\rangle V_{\mu',\mu}(R,\theta,\phi)\langle\lambda,\mu|, \quad (32)$$

where $\mu_{AB}$ is the reduced mass of the complex and $A=-2D_{SO}/3$ is the spin–orbit coupling constant of the F($^2P$) atom. The operators $\hat{\boldsymbol{\lambda}}$ and $\hat{\boldsymbol{S}}$ are the orbital and spin angular momentum of the F-atom, $\hat{\boldsymbol{j}}_A=\hat{\boldsymbol{\lambda}}+\hat{\boldsymbol{S}}$ represents the total atomic angular momentum. The operator $\hat{\boldsymbol{j}}_B$ is the rotational angular momentum of the $H_2$ molecule and $\hat{\boldsymbol{J}}$ the total angular momentum of the complex. The diabatic states of the F($^2P$)–$H_2$ complex that correlate with the corresponding states of the F($^2P$) atom are labeled with the quantum numbers ($\lambda$, $\mu$), where $\lambda=1$ and $\mu=-1,\ 0,\ 1$ is the projection of $\hat{\boldsymbol{\lambda}}$ on the BF $z$-axis $\boldsymbol{R}$. The potentials $V_{\mu',\mu}(R,\theta,\phi)$ are the diabatic interaction potentials in a two-angle embedded BF frame described in Sec. II, Eq. (18). The expansion coefficients are the same as in the three-angle embedded frame, cf. Eq. (9). These expansion coefficients are obtained from the expansion of the three-dimensional potentials in Sec. IV by fixing $r$ at the values mentioned above.

Because of the large spin–orbit coupling $D_{SO}=404$ cm$^{-1}$ of F($^2P$) we used a coupled atomic basis set,

$$|j_A\omega_A\rangle\equiv|(\lambda S)j_A\omega_A\rangle$$
$$=\sum_{\mu,\sigma}|\lambda,\mu\rangle|S,\sigma\rangle\langle\lambda,\mu;S,\sigma|j_A,\omega_A\rangle \quad (33)$$

in which the spin–orbit term in the Hamiltonian $\hat{\boldsymbol{\lambda}}\cdot\hat{\boldsymbol{S}}=(\hat{j}_A^2-\hat{\lambda}^2-\hat{S}^2)/2$ is diagonal. Since $\lambda=1$ and $S=\frac{1}{2}$, one finds that $j_A=\frac{1}{2}$ or $\frac{3}{2}$. The two-angle embedded BF basis for the complex reads

$$|n,j_A,\omega_A,j_B,\omega_B,\Omega\rangle$$
$$=|n\rangle\left[\frac{2J+1}{4\pi}\right]^{1/2}|j_A\omega_A\rangle Y_{j_B,\omega_B}(\theta,\phi)D^{(J)}_{M,\Omega}(\alpha,\beta,0)^*. \quad (34)$$

The spherical harmonics $Y_{j_B,\omega_B}(\theta,\phi)$ describe the rotation of the $H_2$ monomer and the symmetric rotor functions $D^{(J)}_{M,\Omega}(\alpha,\beta,0)^*$ the overall rotation of the complex. The exact quantum numbers $J,M$ are omitted from the shorthand notation on the left-hand side. Remember that ($\beta$, $\alpha$) are the polar angles of the BF $z$-axis $\boldsymbol{R}$ with respect to a SF coordinate system. The components along this axis obey the relation $\Omega=\omega_A+\omega_B$. The radial basis functions $|n\rangle=\chi_n(R)$ are Morse oscillator type functions defined in Ref. 37.

The matrix elements of the Hamiltonian in Eq. (32) over the basis in Eq. (34) are

$$\begin{aligned}
&\langle n',j'_A,\omega'_A,j'_B,\omega'_B,\Omega'|\hat{H}|n,j_A,\omega_A,j_B,\omega_B,\Omega\rangle \\
&\quad=\delta_{j'_A,j_A}\delta_{j'_B,j_B}\delta_{\omega'_A,\omega_A}\delta_{\omega'_B,\omega_B}\delta_{\Omega',\Omega}\Bigg[\langle n'|\frac{-\hbar^2}{2\mu_{AB}R}\frac{\partial^2}{\partial R^2}R|n\rangle+\langle n'|\frac{1}{2\mu_{AB}R^2}|n\rangle(j_A(j_A+1)+j_B(j_B+1)+J(J+1) \\
&\qquad-\omega_A^2-\omega_B^2-\Omega^2)+\delta_{n',n}\{b_0 j_B(j_B+1)+\tfrac{1}{2}A(j_A(j_A+1)-\lambda(\lambda+1)-S(S+1))\}\Bigg] \\
&\qquad+\delta_{j'_A,j_A}\delta_{j'_B,j_B}\langle n'|\frac{1}{2\mu_{AB}R^2}|n\rangle[C^{j_A}_{\omega'_A,\omega_A+1}C^{j_B}_{\omega'_B,\omega_B-1}+C^{j_A}_{\omega'_A,\omega_A-1}C^{j_B}_{\omega'_B,\omega_B+1}-C^{J}_{\Omega',\Omega+1}(C^{j_A}_{\omega'_A,\omega_A+1}+C^{j_B}_{\omega'_B,\omega_B+1}) \\
&\qquad-C^{J}_{\Omega',\Omega-1}(C^{j_A}_{\omega'_A,\omega_A-1}+C^{j_B}_{\omega'_B,\omega_B-1})]+\sum_{\mu',\mu}\langle n',j'_A,\omega'_A,j'_B,\omega'_B,\Omega'|\lambda,\mu'\rangle V_{\mu',\mu}(R,\theta,\phi)\langle\lambda,\mu|n,j_A,\omega_A,j_B,\omega_B,\Omega\rangle
\end{aligned} \tag{35}$$

with $C^{j}_{\omega',\omega\pm1}=\delta_{\omega',\omega\pm1}[j(j+1)-\omega(\omega\pm1)]^{1/2}$.

The expansion of the diabatic potential surfaces $V_{\mu',\mu}(R,\theta,\phi)$ in terms of Racah normalized spherical harmonics $C_{l,m}(\theta,\phi)$ is given by Eq. (18). With Eq. (33) for the coupled atomic basis the potential matrix elements are

$$\begin{aligned}
&\langle n',j'_A,\omega'_A,j'_B,\omega'_B,\Omega'|\lambda,\mu'\rangle V_{\mu',\mu}(R,\theta,\phi)\langle\lambda,\mu|n,j_A,\omega_A,j_B,\omega_B,\Omega\rangle \\
&\quad=(-1)^{2(\lambda-S)+\omega'_B+\omega'_A+\omega_A}[(2j'_A+1)(2j_A+1)(2j'_B+1)(2j_B+1)]^{1/2} \\
&\qquad\times\begin{pmatrix}\lambda & S & j'_A\\ \mu' & \sigma & -\omega'_A\end{pmatrix}\begin{pmatrix}\lambda & S & j_A\\ \mu & \sigma & -\omega_A\end{pmatrix}\sum_{l_B}\langle n'|v^{\mu',\mu}_{l_B}(R)|n\rangle\begin{pmatrix}j'_B & l_B & j_B\\ 0 & 0 & 0\end{pmatrix}\begin{pmatrix}j'_B & l_B & j_B\\ -\omega'_B & \mu-\mu' & \omega_B\end{pmatrix}.
\end{aligned} \tag{36}$$

In addition to $J$ and $M$ there are two exact quantum numbers; the parity of the states of the complex under inversion $\hat{i}$ and the even/odd parity of $j_B$. Even $j_B$ refers to para-$H_2$, odd $j_B$ to ortho-$H_2$ states. The effect of inversion on the basis is

$$\begin{aligned}
&\hat{i}|n,j_A,\omega_A,j_B,\omega_B,\Omega\rangle \\
&\quad=(-1)^{\lambda-j_A+J}|n,j_A,-\omega_A,j_B,-\omega_B,-\Omega\rangle.
\end{aligned} \tag{37}$$

This property can be used to construct a parity-adapted basis or to inspect the parity of the wave functions obtained by diagonalization of the Hamiltonian matrix when the basis is not parity-adapted beforehand.

*Computational details*: The bound states were obtained from a full diagonalization of the Hamiltonian matrix using the LAPACK routines of MATLAB 6 (Ref. 38) and optimization toolboxes. Calculations were performed for $J$ up to $\frac{11}{2}$ inclusive, which provides all the bound states. The levels were converged to within about $10^{-4}$ cm$^{-1}$ with a basis truncated at $j_{B_{max}}=5$. This gives $j_B=0,\ 2,\ 4$ for para-$H_2$ and

TABLE I. Bound states of F–$H_2$ for $J=\frac{1}{2}$ up to $\frac{11}{2}$. Energies are in cm$^{-1}$ relative to the energy of separated F($^2P_{3/2}$) and $H_2(j=0)$ in the case of para states and $H_2(j=1)$ for ortho states. Parities $(+/-)$ of the eigenstates are indicated in parentheses.

| $J=\frac{1}{2}$ | $J=\frac{3}{2}$ | $J=\frac{5}{2}$ | $J=\frac{7}{2}$ | $J=\frac{9}{2}$ | $J=\frac{11}{2}$ |
|---|---|---|---|---|---|
| para-$H_2$ | | | | | |
| −14.568 (+) | −14.086 (−) | −12.179 (+) | −8.907 (−) | −4.414 (+) | |
| −11.460 (−) | −8.367 (+) | −4.802 (−) | −0.864 (+) | | |
| | −3.912 (−) | −1.050 (+) | | | |
| | −3.515 (+) | | | | |
| ortho-$H_2$ | | | | | |
| −18.140 (−) | −19.287 (−) | −17.644 (+) | −14.728 (−) | −10.642 (+) | −5.525 (−) |
| −17.442 (+) | −19.227 (+) | −17.098 (−) | −13.393 (+) | −8.287 (−) | −2.039 (+) |
| −8.431 (+) | −14.632 (+) | −10.841 (−) | −6.755 (+) | −2.340 (−) | |
| −6.731 (−) | −13.230 (−) | −8.576 (+) | −3.967 (−) | | |
| −0.074 (+) | −7.586 (−) | −4.941 (+) | −1.216 (−) | | |
| | −7.094 (+) | −4.273 (+) | −0.031 (−) | | |
| | −6.820 (−) | −4.245 (−) | | | |
| | −4.129 (+) | −0.893 (−) | | | |
| | | −0.756 (+) | | | |
| | | −0.707 (−) | | | |

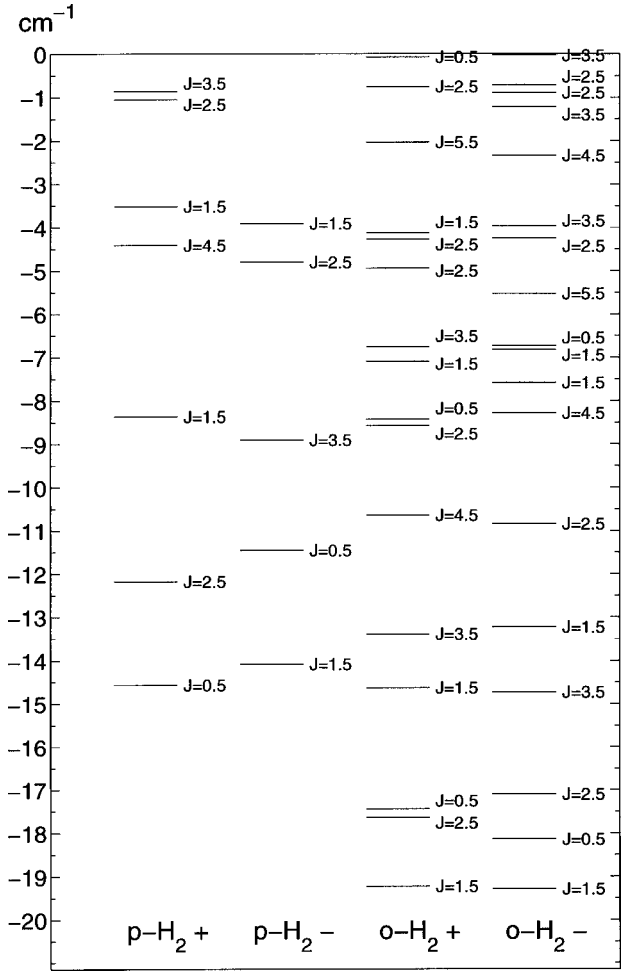


FIG. 4. Bound levels of F($^2P$)–$H_2$ for para and ortho $H_2$ and both ± parities.

$j_B=1,\ 3,\ 5$ for ortho-$H_2$. The radial basis $\chi_n(R)$ consisted of 50 functions ($n_{max}=49$); the nonlinear parameters $R_e=13.5\ a_0$, $D_e=132.5\ cm^{-1}$, and $\omega_e=35.0\ cm^{-1}$ in this basis were optimized in energy minimizations with smaller values of $n_{max}$.

We tested our program by constructing simple model diabatic potentials that consist of an isotropic Morse potential and the anisotropic electrostatic quadrupole–quadrupole term. This model produces directly the analytical form of the diabatic potentials $V_{\mu',\mu}(R,\theta,\phi)$ for all $\mu'$ and $\mu=-1,\ 0,\ 1$, see Eq. (22) in Sec. III. We coded the computation of the Hamiltonian matrix and its eigenvalues in a fully coupled basis in space-fixed coordinates with the formulas from Refs. 4 and 5, as well as in the spin–orbit coupled BF basis of Eqs. (33) and (34). The eigenvalues agree to machine accuracy. Furthermore, we performed the calculation of the bound levels in this model potential and the levels of F–$H_2$ with the HIBRIDON 4.1 (Ref. 39) suite of programs. The definitions of the diabatic potentials that HIBRIDON needs as input are given in Ref. 3. We discovered that the potential $V_{xz}(R,\theta)$ occurring in Table I of Ref. 3 should be divided by $2^{1/2}$ instead of multiplied by this factor, and that the HIBRIDON input potential $V_d(R,\theta)$ does not correspond to $(V_{yy}-V_{xx})/2$ as in Eq. (23) of Ref. 3 but, instead, to $(V_{xx}-V_{yy})/2$. With these changes in the input HIBRIDON produced results that were in perfect agreement with those from our programs.

## VI. RESULTS AND DISCUSSION

The complete set of rovibrational energies of the F–$H_2$ van der Waals complex is given in Table I. Figure 4 represents the levels graphically. The potential that we used pro-

TABLE II. Character of the bound states in Table I for $J=\frac{1}{2}$ up to $\frac{5}{2}$, in terms of the parity-adapted basis with quantum numbers $||\omega_A|,|\omega_B|,|\Omega|,\pm\rangle$. All these low lying states have $j_A=\frac{3}{2}$, with $j_B=0$ for para-$H_2$ and $j_B=1$ for ortho-$H_2$. Only the most important basis functions are indicated. The label ± denotes the overall parity of the eigenvector.

| $J=\frac{1}{2}$ | $J=\frac{3}{2}$ | $J=\frac{5}{2}$ |
|---|---|---|
| para-$H_2$ | | |
| 99% $\lvert\frac{1}{2},0,\frac{1}{2},+\rangle$ | 96% $\lvert\frac{1}{2},0,\frac{1}{2},-\rangle$ | 93% $\lvert\frac{1}{2},0,\frac{1}{2},+\rangle$ |
| 99% $\lvert\frac{1}{2},0,\frac{1}{2},-\rangle$ | 86% $\lvert\frac{1}{2},0,\frac{1}{2},+\rangle$ | 60% $\lvert\frac{1}{2},0,\frac{1}{2},-\rangle$, 40% $\lvert\frac{3}{2},0,\frac{3}{2},-\rangle$ |
| | 97% $\lvert\frac{3}{2},0,\frac{3}{2},-\rangle$ | 93% $\lvert\frac{3}{2},0,\frac{3}{2},+\rangle$ |
| | 87% $\lvert\frac{3}{2},0,\frac{3}{2},+\rangle$ | |
| ortho-$H_2$ | | |
| 96% $\lvert\frac{1}{2},1,\frac{1}{2},-\rangle$ | 66% $\lvert\frac{1}{2},1,\frac{3}{2},-\rangle$, 28% $\lvert\frac{1}{2},1,\frac{1}{2},-\rangle$ | 58% $\lvert\frac{1}{2},1,\frac{3}{2},+\rangle$, 30% $\lvert\frac{1}{2},1,\frac{1}{2},+\rangle$ |
| 98% $\lvert\frac{1}{2},1,\frac{1}{2},+\rangle$ | 60% $\lvert\frac{1}{2},1,\frac{3}{2},+\rangle$, 37% $\lvert\frac{1}{2},1,\frac{1}{2},+\rangle$ | 55% $\lvert\frac{1}{2},1,\frac{3}{2},-\rangle$, 40% $\lvert\frac{1}{2},1,\frac{1}{2},-\rangle$ |
| 69% $\lvert\frac{1}{2},0,\frac{1}{2},+\rangle$, 31% $\lvert\frac{3}{2},1,\frac{1}{2},+\rangle$ | 55% $\lvert\frac{1}{2},1,\frac{1}{2},+\rangle$, 31% $\lvert\frac{1}{2},1,\frac{3}{2},+\rangle$ | 44% $\lvert\frac{1}{2},1,\frac{1}{2},-\rangle$, 24% $\lvert\frac{1}{2},1,\frac{3}{2},-\rangle$, 17% $\lvert\frac{3}{2},0,\frac{3}{2},-\rangle$ |
| 54% $\lvert\frac{1}{2},0,\frac{1}{2},-\rangle$, 46% $\lvert\frac{3}{2},1,\frac{1}{2},-\rangle$ | 69% $\lvert\frac{1}{2},1,\frac{1}{2},-\rangle$, 22% $\lvert\frac{1}{2},1,\frac{3}{2},-\rangle$ | 57% $\lvert\frac{1}{2},1,\frac{1}{2},+\rangle$, 15% $\lvert\frac{3}{2},0,\frac{3}{2},+\rangle$ |
| 77% $\lvert\frac{3}{2},1,\frac{1}{2},+\rangle$, 21% $\lvert\frac{1}{2},0,\frac{1}{2},+\rangle$ | 51% $\lvert\frac{3}{2},0,\frac{3}{2},-\rangle$, 34% $\lvert\frac{1}{2},0,\frac{1}{2},-\rangle$ | 60% $\lvert\frac{3}{2},0,\frac{3}{2},+\rangle$, 22% $\lvert\frac{1}{2},1,\frac{3}{2},+\rangle$ |
| | 90% $\lvert\frac{3}{2},0,\frac{3}{2},+\rangle$ | 52% $\lvert\frac{1}{2},0,\frac{1}{2},+\rangle$, 27% $\lvert\frac{3}{2},1,\frac{1}{2},+\rangle$ |
| | 39% $\lvert\frac{3}{2},0,\frac{3}{2},-\rangle$, 35% $\lvert\frac{1}{2},0,\frac{1}{2},-\rangle$, 27% $\lvert\frac{3}{2},1,\frac{1}{2},-\rangle$ | 70% $\lvert\frac{3}{2},0,\frac{3}{2},-\rangle$, 14% $\lvert\frac{1}{2},1,\frac{3}{2},-\rangle$ |
| | 56% $\lvert\frac{3}{2},1,\frac{1}{2},+\rangle$, 43% $\lvert\frac{1}{2},0,\frac{1}{2},+\rangle$ | 87% $\lvert\frac{3}{2},1,\frac{5}{2},-\rangle$ |
| | | 84% $\lvert\frac{3}{2},1,\frac{5}{2},+\rangle$ |
| | | 65% $\lvert\frac{3}{2},1,\frac{1}{2},-\rangle$, 29% $\lvert\frac{1}{2},0,\frac{1}{2},-\rangle$ |

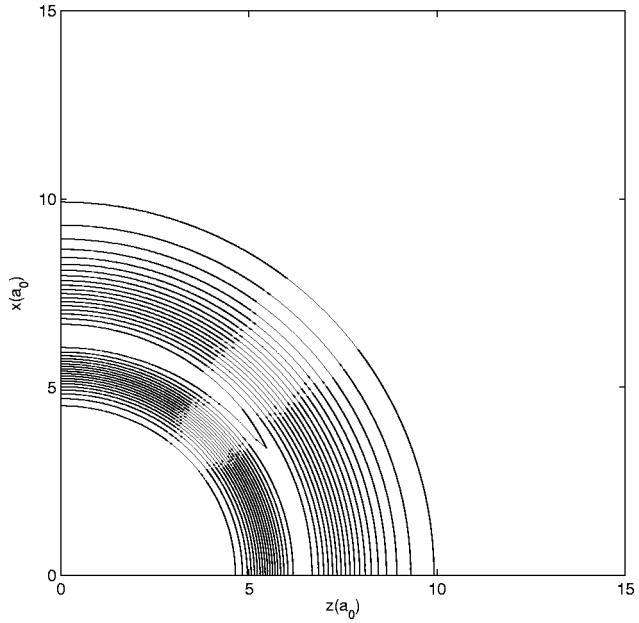


FIG. 5. Density of the $J=\frac{1}{2}$ bound state of para-$H_2$–F of + parity as function of the F-atom position in the BF $xz$ plane, with the hydrogen molecule lying along the horizontal $z$ axis and the origin at the center-of-mass of $H_2$. Energy: $-14.570\ \mathrm{cm}^{-1}$.

duces no bound states for quantum numbers $J$ larger than $\frac{9}{2}$ for para-$H_2$ and for $J$ larger than $\frac{11}{2}$ for ortho-$H_2$. The binding energy $D_0$ of the para-$H_2$ complex is $14.6\ \mathrm{cm}^{-1}$; the ortho-$H_2$ complex is bound by $19.3\ \mathrm{cm}^{-1}$. For comparison we note that the well depth $D_e$ of the lowest adiabatic potential (with $\theta=90°$) is $141.4\ \mathrm{cm}^{-1}$ and the well depth of the lowest adiabatic potential with the spin–orbit coupling included is $67.8\ \mathrm{cm}^{-1}$ (also for $\theta=90°$).[25] Hence, this complex contains a substantial amount of zero-point energy.

In order to test the effect of freezing the $H_2$ bond length at the vibrationally averaged value $r_0=1.44836\ a_0$ we also performed computations with the $H_2$ bond length frozen at $r_e=1.40112\ a_0$ and with the three-dimensional diabatic potentials averaged over the ground vibrational $(v=0)$ wave function of $H_2$. The well depth of the lowest adiabatic potential without spin–orbit coupling is $133.1\ \mathrm{cm}^{-1}$ for $r=r_e$, $141.4\ \mathrm{cm}^{-1}$ for $r=r_0$, and $142.3\ \mathrm{cm}^{-1}$ for the vibrationally averaged case. With the inclusion of spin–orbit coupling the well depths of the lowest adiabatic potential are 64.5, 67.8, and $68.2\ \mathrm{cm}^{-1}$, respectively. The lowest bound levels are higher by about $1.2\ \mathrm{cm}^{-1}$ than the levels reported in Table I and Fig. 4 when we change $r$ from $r_0$ to $r_e$ and lower by about $0.2\ \mathrm{cm}^{-1}$ for the vibrationally averaged potential. These changes become smaller when the levels approach the dissociation threshold. Especially the changes in going from $r_e$ to $r_0$ are substantial; this is related to the presence of a chemically bound energy minimum for the linear F–H–H geometry. The depth of this chemical minimum and the barrier that separates it from the van der Waals minimum are strongly dependent on $r$ (Ref. 25) and also the depth of the latter minimum depends rather sensitively on $r$.

Takayanagi and Kurosaki[24] reported van der Waals resonances in the cumulative reaction probabilities for the F–$H_2$

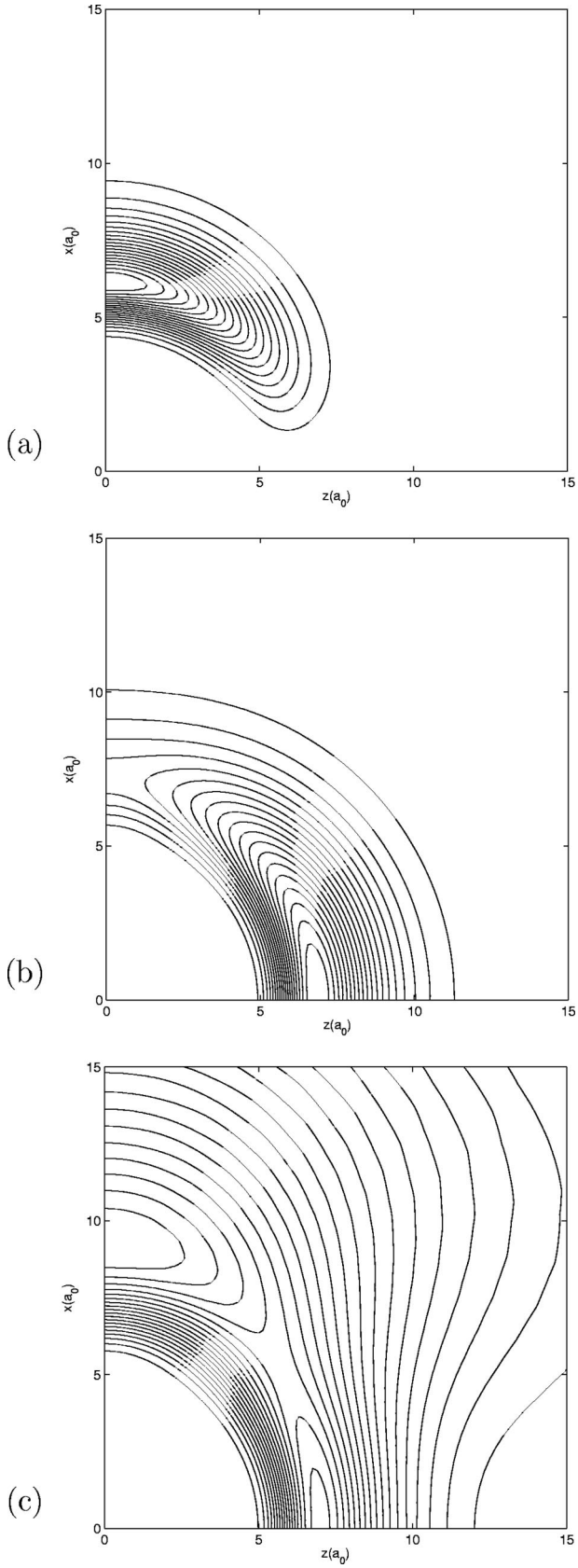


FIG. 6. Density of the $J=\frac{1}{2}$ bound states of ortho-$H_2$–F of + parity as function of the F-atom position in the BF $xz$ plane, with the hydrogen molecule lying along the horizontal $z$ axis and the origin at the center-of-mass of $H_2$. Energies: (a) $-17.442$, (b) $-8.431$, (c) $-0.074\ \mathrm{cm}^{-1}$.

TABLE III. Bound states of F–$H_2$ for $J=\frac{1}{2}$ up to $\frac{13}{2}$ calculated with the potential of Aquilanti *et al.* (Ref. 17). Explanations, see Table I.

| $J=\frac{1}{2}$ | $J=\frac{3}{2}$ | $J=\frac{5}{2}$ | $J=\frac{7}{2}$ | $J=\frac{9}{2}$ | $J=\frac{11}{2}$ | $J=\frac{13}{2}$ |
|---|---|---|---|---|---|---|
| para-$H_2$ | | | | | | |
| −17.800 (+) | −17.258 (−) | −15.308 (+) | −11.986 (−) | −7.381 (+) | −1.672 (−) | |
| −14.768 (−) | −11.423 (+) | −7.190 (−) | −2.429 (+) | | | |
| | −3.869 (−) | −1.198 (+) | | | | |
| | −3.699 (+) | −0.487 (−) | | | | |
| ortho-$H_2$ | | | | | | |
| −22.795 (−) | −23.877 (−) | −22.094 (+) | −18.976 (−) | −14.621 (+) | −9.145 (−) | −2.725 (+) |
| −22.270 (+) | −23.868 (+) | −21.757 (−) | −18.071 (+) | −12.925 (−) | −6.467 (+) | |
| −9.205 (+) | −19.019 (+) | −14.610 (−) | −9.499 (+) | −4.019 (−) | | |
| −7.484 (−) | −17.978 (−) | −12.786 (+) | −6.833 (−) | −0.884 (+) | | |
| −0.445 (+) | −8.249 (−) | −5.984 (+) | −2.369 (−) | | | |
| −0.005 (−) | −6.168 (+) | −4.265 (+) | −1.266 (−) | | | |
| | −6.126 (−) | −4.180 (−) | −0.837 (+) | | | |
| | −4.903 (+) | −1.467 (−) | | | | |
| | | −1.125 (−) | | | | |
| | | −1.057 (+) | | | | |

system. In order to characterize these resonances they employed the Stark–Werner potential[40] for F–$H_2$, obtained one-dimensional potential curves by averaging the diabatic potentials over the $^2P_{3/2}$ ground state of the free F-atom and over the rovibrational states $(v,j)$ of free $H_2$, and then solved the one-dimensional Schrödinger equation for each curve separately. From Fig. 3 of their paper[24] one can estimate their value of $D_0$. It is 12–14 $cm^{-1}$ for the para-$H_2$ complex which, in spite of their approximations, is quite close to our result. But they find a substantially smaller value of $D_0$ for the ortho-$H_2$ complex, whereas we find a larger value. This must be due to their rotational averaging over the unperturbed $j=1$ state of ortho-$H_2$, while in our treatment the ortho-$H_2$ monomer can use its $\omega=-1$, 0, 1 components to adopt the most favorable orientation in the complex.

Table II gives the character of the eigenvectors for $J=\frac{1}{2}$, $\frac{3}{2}$, and $\frac{5}{2}$ expressed in the spin–orbit coupled basis and Figs. 5 and 6 show density contours of the $J=\frac{1}{2}$ bound states of the para and ortho $H_2$–F complex. These densities are obtained by integration of the absolute square of the wave function over all coordinates except $R$ and $\theta$. They are displayed as functions of $z=R\cos\theta$ and $x=R\sin\theta$, the Cartesian coordinates of the F atom, with the horizontal $z$ axis representing the $H_2$ bond axis and the origin at the center of mass of the hydrogen molecule. We show only the densities of the bound states of + parity, as there is very little difference with the corresponding states of − parity. In Fig. 5 one observes that the para-$H_2$ molecule in the F–$H_2$ complex is very nearly spherical, in agreement with the observation in Table II that the bound state wave function has almost exclusively $j_B=0$ character and little admixture of the basis functions with higher (even) $j_B$. This is a consequence of the large rotational constant $b_0=59.34$ $cm^{-1}$ of $H_2$, which causes a gap of 356 $cm^{-1}$ between the levels with $j_B=2$ and $j_B=0$ that is large with respect to the anisotropy in the F–$H_2$ potential.

Also the bound states of ortho-$H_2$–F contain almost exclusively the lowest rotational $H_2$ wave function which has $j_B=1$ in this case. Since the $j_B=1$ state has degenerate components with $\omega_B=-1$, 0, 1, the $H_2$ molecule in the bound ortho-$H_2$–F complex has the possibility to adopt its most favorable orientation. Figure 6(a) shows that a T-shaped complex with primarily $|\omega_B|=1$ (see Table II) has the lowest energy. It is somewhat more compact, with maximum density at $R=6.19\,a_0$, than the bound state of para-$H_2$–F with maximum density at $R=6.31\,a_0$. This is in agreement with the binding energy $D_0$ being larger for ortho-$H_2$–F than for para-$H_2$–F; the states with $J=\frac{1}{2}$ and + parity that are displayed lie at −17.4 and −14.6 $cm^{-1}$, respectively. The next higher ortho-$H_2$–F bound state with $J=\frac{1}{2}$ has mainly $\omega_B=0$ character with some admixture of $|\omega_B|=1$ components and it adopts primarily the linear geometry, see Fig. 6(b), with maximum density at $R=6.85\,a_0$. The highest level of ortho-$H_2$–F is bound by only 0.074 $cm^{-1}$ and it is quite diffuse. Figure 6(c) shows that it has two maxima in the density, one for the T-shaped geometry at $R=9.31\,a_0$ and one for the linear geometry at $R=6.99\,a_0$. For higher $J$ values the densities do not present new features. The radius of maximum density changes slightly from one state to another but the pattern observed for $J=\frac{1}{2}$ remains.

The electronic quantum number corresponding to these low lying states is always $j_A=\frac{3}{2}$. The large spin–orbit splitting in the F($^2P$) atom makes the $j_A=\frac{1}{2}$ states nearly inaccessible. The $\omega_A$ quantum number which corresponds to the projection of $j_A$ on the intermolecular axis $\boldsymbol{R}$ may vary from one state to another, however. The para-$H_2$–F bound state with $J=\frac{1}{2}$ must have $|\omega_A|=\frac{1}{2}$ because $j_B=\omega_B=0$ for this state and $\Omega=\omega_A+\omega_B$ must be $\pm\frac{1}{2}$ for $J=\frac{1}{2}$. For the para-$H_2$–F states with $J\geqslant\frac{3}{2}$ and for the ortho-$H_2$–F states $|\omega_A|$ can be either $\frac{1}{2}$ or $\frac{3}{2}$. Table II shows that most of the lower bound states have $|\omega_A|=\frac{1}{2}$, whereas the higher states obtain more and more $|\omega_A|=\frac{3}{2}$ character. This quantum number $|\omega_A|$ is related to the orientation of the "$p$-hole" in the electron distribution of the F($^2P$) atom. For $|\omega_A|=\frac{3}{2}$ the projection of the orbital angular momentum $\lambda=1$ can only be $\mu=\pm1$ and, hence, the $p$-hole is directed perpendicular to the F–$H_2$ axis $\boldsymbol{R}$. States with $|\omega_A|=\frac{1}{2}$ and $j_A=\frac{3}{2}$ contain two-

thirds of the $\mu=0$ character and one-third of the $\mu=\pm 1$ character, cf. Eq. (33), and the $p$-hole is primarily directed along $\boldsymbol{R}$ for such states.

Table III lists the energies of the bound levels computed with the empirical potential of Aquilanti *et al.*[17] They are lower than the levels in Table I and Fig. 4 and $D_0$ is larger, due to the deeper well in the diabatic potential $V_{0,0}$. Also the number of bound states is larger for this potential. Additional bound states appear for $J=\frac{11}{2}$ in para-$H_2-F$ and for $J=\frac{13}{2}$ in ortho-$H_2-F$. We also analyzed the bound wave functions; most of them are similar to the eigenvectors reported in Table II.

At present, there are no experimental data to compare with our predicted levels. We hope that spectroscopists will soon acquire these data. Since the levels depend sensitively on the potential surface, one will then be able to tell which of the potentials is the most accurate. Finally we mention that similar work on the bound states of $Cl(^2P)-H_2$, $Br(^2P)-H_2$, and $Cl(^2P)-HCl$ is in progress. Also inelastic scattering and photodissociation cross sections are being calculated. All this work makes use of the procedures outlined in the present paper and the diabatic potentials of Kłos *et al.*[30,41,42] calculated with the UCCSD(T) method.

## ACKNOWLEDGMENTS

This research has been financially supported by the Council for Chemical Sciences of the Netherlands Organization for Scientific Research (CW-NWO). We also acknowledge support from the European Research Training Network THEONET II. We thank Professor V. Aquilanti and Dr. A. Volpi for sending us the code of their $F-H_2$ potential and Dr. P. E. S. Wormer for critically reading the manuscript and useful comments.

[1] A. van der Avoird, P. E. S. Wormer, F. Mulder, and R. M. Berns, Top. Curr. Chem. **93**, 1 (1980).
[2] A. van der Avoird, P. E. S. Wormer, and R. Moszynski, Chem. Rev. **94**, 1931 (1994).
[3] M. H. Alexander, J. Chem. Phys. **99**, 6014 (1993).
[4] M.-L. Dubernet and J. Hutson, J. Chem. Phys. **101**, 1939 (1994).
[5] M.-L. Dubernet and J. Hutson, J. Phys. Chem. **98**, 5844 (1994).
[6] D. E. Manolopoulos, J. Chem. Soc., Faraday Trans. **93**, 673 (1997).
[7] M. H. Alexander, D. E. Manolopoulos, and H.-J. Werner, J. Chem. Phys. **113**, 11084 (2000).
[8] D. E. Manolopoulos, K. Stark, H.-J. Werner, D. W. Arnold, S. E. Bradforth, and D. M. Neumark, Science **262**, 1852 (1993).
[9] J. F. Castillo, B. Hartke, H.-J. Werner, F. J. Aoiz, B. Bañares, and B. Martìnez-Haya, J. Chem. Phys. **109**, 7224 (1998).
[10] J. F. Castillo, D. E. Manolopoulos, K. Stark, and H.-J. Werner, J. Chem. Phys. **104**, 6531 (1996).
[11] M. Baer, M. Faubel, B. Martinez-Haya, L. Y. Rusin, U. Tappe, and J. P. Toennies, J. Chem. Phys. **104**, 2743 (1996).
[12] P. Honvault and J.-M. Launay, Chem. Phys. Lett. **270**, 287 (1998).
[13] P. Honvault and J.-M. Launay, Chem. Phys. Lett. **303**, 657 (1999).
[14] J. F. Castillo and D. E. Manolopoulos, Faraday Discuss. **110**, 119 (1998).
[15] R. T. Skodje, D. Skouteris, D. E. Manolopoulos, S. H. Lee, F. Dong, and K. Liu, J. Chem. Phys. **112**, 4536 (2000).
[16] V. Aquilanti, R. Candori, D. Cappelletti, E. Luzzatti, and F. Pirani, Chem. Phys. **145**, 293 (1990).
[17] V. Aquilanti, S. Cavalli, F. Pirani, A. Volpi, and D. Cappelletti, J. Phys. Chem. A **105**, 2401 (2001).
[18] V. Aquilanti, S. Cavalli, D. D. Fazio, A. Volpi, A. Aquilar, X. Giménez, and J. M. Lucas, Phys. Chem. Chem. Phys. **4**, 401 (2002).
[19] M. Faubel, L. Y. Rusin, S. Schlemmer, F. Sondermann, U. Tappe, and J. P. Toennies, J. Chem. Soc., Faraday Trans. **89**, 1475 (1993).
[20] F. A. Gianturco, F. Ragnetti, M. Faubel, B. Martínez-Haya, L. Y. Rusin, F. Sondermann, and U. Tappe, Chem. Phys. **200**, 405 (1995).
[21] M. Ayabakan, M. Faubel, B. Martínez-Haya, L. Y. Rusin, M. B. Sevryuk, U. Tappe, and J. P. Toennies, Chem. Phys. **229**, 21 (1998).
[22] D. Skouteris, D. E. Manolopoulos, W. Bian, H. J. Werner, L.-H. Lai, and K. Liu, Science **286**, 1713 (1999).
[23] F. J. Aoiz, L. Bañares, J. F. Castillo, M. Menéndez, D. Skouteris, and H.-J. Werner, J. Chem. Phys. **115**, 2074 (2001).
[24] T. Takayanagi and Y. Kurosaki, J. Chem. Phys. **109**, 8929 (1998).
[25] J. Kłos, G. Chałasiński, and M. M. Szczęśniak, Int. J. Quantum Chem. **90**, 1038 (2002).
[26] D. M. Brink and G. R. Satchler, *Angular Momentum*, 3rd ed. (Clarendon, Oxford, 1993).
[27] G. Brocks, A. van der Avoird, B. T. Sutcliffe, and J. Tennyson, Mol. Phys. **50**, 1025 (1983).
[28] M. C. G. N. van Vroonhoven and G. C. Groenenboom, J. Chem. Phys. **117**, 5240 (2002).
[29] A. J. H. M. Meijer, G. C. Groenenboom, and A. van der Avoird, J. Chem. Phys. **101**, 7603 (1994).
[30] J. Kłos, G. Chałasiński, and M. M. Szczęśniak, J. Chem. Phys. **117**, 4709 (2002).
[31] A. D. Esposti and H.-J. Werner, J. Chem. Phys. **93**, 3351 (1990).
[32] J. W. Riehl, C. J. Fischer, J. D. Baloga, and J. L. Kinsey, J. Chem. Phys. **58**, 4571 (1973).
[33] R. J. Le Roy and J. van Kranendonk, J. Chem. Phys. **61**, 4750 (1974).
[34] U. Buck, H. Meyer, and R. J. Le Roy, J. Chem. Phys. **80**, 5589 (1984).
[35] R. J. Le Roy and J. M. Hutson, J. Chem. Phys. **86**, 837 (1987).
[36] M. Jeziorska, P. Jankowski, K. Szalewicz, and B. Jeziorski, J. Chem. Phys. **113**, 2957 (2000).
[37] J. Tennyson and B. T. Sutcliffe, J. Chem. Phys. **77**, 4061 (1982).
[38] MATLAB Version 6, The MathWorks, Inc., 24 Prime Park Way, Natick, MA (1996), http://www.mathworks.com/
[39] HIBRIDON is a package of programs for the time-independent quantum treatment of inelastic collisions and photodissociation written by M. H. Alexander, D. Manolopoulos, H.-J. Werner, and B. Follmeg, with contributions by P. Vohralik, G. Corey, B. Johnson, T. Orlikowski, and P. Valiron.
[40] K. Stark and H.-J. Werner, J. Chem. Phys. **104**, 6515 (1996).
[41] J. Kłos, G. Chałasiński, and M. M. Szczęśniak, J. Phys. Chem. **106**, 7362 (2002).
[42] J. Kłos, G. Chałasiński, M. M. Szczęśniak, and H.-J. Werner, J. Chem. Phys. **115**, 3085 (2001).